

---

D.V. KONDRYUK, V.M. KRAMAR

Yu. Fed'kovych Chernivtsi National University

(2, Kotsyubyns'kyi Str., Chernivtsi 58012, Ukraine; e-mail: v.kramar@chnu.edu.ua)

**THICKNESS, CONCENTRATION,  
AND TEMPERATURE DEPENDENCES  
OF EXCITON TRANSITION ENERGIES  
IN  $\text{Al}_x\text{Ga}_{1-x}\text{As}/\text{GaAs}/\text{Al}_x\text{Ga}_{1-x}\text{As}$  NANOFILMS**

PACS 71.35.Cc; 72.20.Mf;  
78.67.De

---

*The energy of transition into the ground excitonic state for a quasi-two-dimensional (nanofilm) semiconductor nanoheterostructure with single quantum well and its dependences on the thickness, temperature, and composition of the barrier medium are calculated in the dielectric continuum approximation using the Green's function method. Specific calculations are made for a nanofilm containing a rectangular finite-depth quantum well created by the double heterojunction  $\text{GaAs}/\text{Al}_x\text{Ga}_{1-x}\text{As}$  taken as an example. For the films narrower than 30–40 nm, the transition energy is shown to be mainly governed by the confinement effect and the aluminum content  $x$ . In particular, the energy decreases rapidly from 1.55 eV (at  $x = 0.2$ ), 1.62 eV (at  $x = 0.3$ ), or 1.69 eV (at  $x = 0.4$ ) to 1.41 eV for all those  $x$ -values, as the film thickness grows. The further increase in the film thickness up to approximately 100 nm is accompanied by a slow growth of the energy to the value characteristic of bulk GaAs, which occurs due to the corresponding reduction in the exciton binding energy. The rate of this growth depends weakly on  $x$ . The temperature increase from 0 to 300 K results in a long-wave shift of the exciton band bottom. As a result, the transition energy decreases by a value weakly depending on the film thickness and ranging from 2 meV at  $x = 0.2$  to 3 meV at  $x = 0.4$ . The temperature-induced variations are invoked by the interaction with phonons, which are mostly confined ones in nanofilms thicker than 30–40 nm or interface ones, if nanofilms are thinner.*

*Keywords:* nanoheterostructure, quantum well, exciton, exciton-phonon coupling.

## 1. Introduction

The issues associated with manufacturing the nano-dimensional crystal structures and studying their electric and optical properties have been a point of keen interest for several decades. They remain challenging till now, owing to the onrush of technologies aimed at fabricating superthin crystal layers. As a result, various semiconductor-based low-dimensional nanoheterostructures, which are suitable for the application as element units in novel electronic and optoelectronic devices, have been created: transistors,

electronic switches, radiation sources and detectors, optical filters, and others. They will favor a reduction in the dimensions and the energy consumption of the devices manufactured on their basis, as well as the productivity enhancement for such devices [1–6]. The most wide-spread elements used in the creation of those devices are structures fabricated on the basis of  $\text{GaAs}/\text{Al}_x\text{Ga}_{1-x}\text{As}$  heterojunction [7–12].

The development and the improvement of nanotechnologies in optoelectronics require the creation of new theoretical models, which would adequately describe the properties of nanostructures. The methods used in theoretical researches of the state of quasi-particles in nanoheterostructures with quantum wells

(QWs) and the interaction between them are well-known [13–21]. They were applied to study the dependences of the electron, hole, and exciton energies in various nanosystems on the dimension and the temperature of the system. In particular, these were flat nanostructures with double heterojunction of the indicated type, namely,  $\text{Al}_x\text{Ga}_{1-x}\text{As}/\text{GaAs}/\text{Al}_x\text{Ga}_{1-x}\text{As}$  nanofilms [20, 21]. However, the dependence of the quasiparticle spectra in similar nanosystems on the content  $x$  of the solid solution (the latter is a material that heterojunction's barriers consist of) has not been analyzed. At the same time, changes in the barrier material composition inevitably transform the electron spectrum of nanoheterostructures, which may turn out an essential tuning factor at designing the quantum cascade lasers and detectors [22, 23].

The indicated problem is a matter of this work. Here, we report the results of our calculations for the dependences of the energy of excitonic transition into the ground state of the  $\text{Al}_x\text{Ga}_{1-x}\text{As}/\text{GaAs}/\text{Al}_x\text{Ga}_{1-x}\text{As}$  nanofilm on the temperature  $T$  and the nanofilm thickness  $a$  for various aluminum contents  $x$  in the barrier medium. In the framework of the dielectric continuum model and the model of single rectangular QW with finite depth, as well as the effective mass and weak exciton-phonon coupling approximations, and using the Green's function method, we analyze the temperature and size dependences of the energy of excitonic transition into the ground excitonic state in flat semiconductor-based nanofilms. Specific calculations were performed, as an example, for the  $\text{Al}_x\text{Ga}_{1-x}\text{As}/\text{GaAs}/\text{Al}_x\text{Ga}_{1-x}\text{As}$  nanofilm with  $x = 0.2, 0.3, \text{ and } 0.4$ . The influence of all phonon spectrum branches on the energy of transition into the ground excitonic nanofilm state was analyzed.

## 2. Discussion of the Model and Statement of the Problem

Let an electron-hole pair move almost freely in the flat semiconductor nanofilm formed by two parallel heterojunctions located at the planes  $z = \pm a/2$  in the Cartesian coordinate system between the well (GaAs) and barrier ( $\text{Al}_x\text{Ga}_{1-x}\text{As}$ ) media. Each quasiparticle is located in its QW and interacts with another one, as well as with its own electrostatic images in both heterojunction planes. The heterojunction is considered to be unstrained, because the GaAs and AlAs compounds have close values of lattice period  $a_0$

(5.653 and 5.661 Å, respectively), as well as static,  $\varepsilon_0$  (13.18 and 10.06, respectively), and high-frequency,  $\varepsilon_\infty$  (10.89 and 8.16, respectively), dielectric permittivities [24]. This fact also allows us to neglect the self-polarization of the heterojunction planes and consider the QW to be rectangular with width  $a$ . In the effective mass approximation, the Hamiltonian of a free exciton in the nanofilm looks like [20]

$$\hat{H}_{\text{ex}} = \hat{H}_e^\perp + \hat{H}_h^\perp + \hat{H}_{\text{SS}} + \hat{H}_p = \hat{H}_0 + \hat{H}_p, \quad (1)$$

where the terms  $\hat{H}_e^\perp$  and  $\hat{H}_h^\perp$  describe the motion of quasiparticles in the direction perpendicular to the heterojunction plane,  $\hat{H}_{\text{SS}}$  is the Shinada–Sugano Hamiltonian,  $\hat{H}_p = \frac{\beta e^2}{\varepsilon \rho} - \frac{e^2}{\varepsilon |\mathbf{r}_e - \mathbf{r}_h|}$  is the perturbation operator that involves the differences between the motions of three- and two-dimensional excitons in the nanofilm medium with the dielectric permittivity  $\varepsilon$ ,  $\boldsymbol{\rho} = \boldsymbol{\rho}_e - \boldsymbol{\rho}_h$ , and  $\beta$  is a variational parameter introduced for the minimization of the exciton steady state energy. Accordingly, the ground-state energy of an exciton in the nanofilm with thickness  $a$  is the sum

$$E_{\text{ex}}^{(0)}(a) = E_g + E_1^{(e)}(a) + E_1^{(h)}(a) - E_b(a), \quad (2)$$

where  $E_g$  is the energy gap width in the well material,  $E_1^{(j)}(a)$  the energy of the lowest quasiparticle minilevel in the QW, and  $E_b(a)$  the exciton binding energy. The methods of their calculation are given in work [20].

In the dielectric continuum model [14], the polarization optical vibrations of atoms in the nanoheterostructure (interaction with them can change the energy spectrum of an exciton) are classified as the systems of phonons confined in the nanofilm volume ( $L0$ ), semiconfined in barriers ( $L1$ ), and interface ( $I$ ) ones. The Hamiltonian of this system is given in works [13, 15].

If the exciton radius considerably exceeds the polaron one, we may consider that the exciton-phonon coupling is realized by means of the phonon interaction with the electron and the hole. Then the Hamiltonian with exciton-phonon coupling reads

$$\begin{aligned} \hat{H}_{\text{int}} = & \hat{H}_{\text{ex}-L0} + \hat{H}_{\text{ex}-L1} + \hat{H}_{\text{ex}-I} = \sum_{j=e,h} \eta_j \times \\ & \times \left[ \sum_{n_j, n'_j, \mathbf{k}_\parallel} \left( \sum_{\lambda, \mathbf{q}_\parallel} F_{n_j n'_j}^\lambda(\mathbf{q}_\parallel) a_{n'_j, \mathbf{k}_\parallel + \mathbf{q}_\parallel}^+ a_{n_j, \mathbf{k}_\parallel} B_{\lambda \mathbf{q}_\parallel} \right) \right] \end{aligned}$$

$$\begin{aligned}
 & + \sum_{q_{\perp}, \mathbf{q}_{\parallel}} F_{n_j n'_j}^{q_{\perp}}(\mathbf{q}_{\parallel}) a_{n'_j \mathbf{k}'_{\parallel} + \mathbf{q}_{\parallel}}^{\dagger} a_{n_j \mathbf{k}_{\parallel}} B_{q_{\perp} \mathbf{q}_{\parallel}} + \\
 & + \sum_{\sigma, p, \mathbf{q}_{\parallel}} F_{n_j n'_j}^{\sigma p}(\mathbf{q}_{\parallel}) a_{n'_j \mathbf{k}'_{\parallel} + \mathbf{q}_{\parallel}}^{\dagger} a_{n_j \mathbf{k}_{\parallel}} B_{\sigma p \mathbf{q}_{\parallel}} \Big) \Big], \quad (3)
 \end{aligned}$$

where  $\eta_e = 1$ ;  $\eta_h = -1$ ;  $a_{n_j \mathbf{k}}^{\dagger}$  and  $a_{n_j \mathbf{k}}$  are the creation and annihilation, respectively, operators for an electron ( $j = e$ ) and a hole ( $j = h$ ) with the wave vector  $\mathbf{k}$  in the  $n_j$ -th band;  $B_{\Lambda \mathbf{q}_{\parallel}} = b_{\Lambda \mathbf{q}_{\parallel}} + b_{\Lambda - \mathbf{q}_{\parallel}}^{\dagger}$ ; the subscript  $\Lambda$  distinguishes the type and simultaneously determines the transverse component  $q_{\perp}$  of the phonon wave vector  $\mathbf{q}$ : confined ( $\Lambda = \lambda$ ), semi-confined ( $\Lambda = q_{\perp}$ ), and interface ( $\Lambda = (\sigma, p)$ ) phonon branches (in the latter case, the subscript  $\sigma$  distinguishes the symmetric ( $\sigma = S$ ) and antisymmetric ( $\sigma = A$ ) branches, and the subscript  $p$  the high- ( $p = +$ ) and low-energy ( $p = -$ ) ones) [15]; and  $F_{n_j n'_j}^{\Lambda}(\mathbf{q}_{\parallel})$  are the functions describing the carrier coupling with the corresponding phonon state. The explicit forms of the coupling function dependences on the nanofilm thickness  $a$  and the longitudinal component  $\mathbf{q}_{\parallel}$  of the wave vector for each type of phonons in double-heterojunction structures are presented in work [15]. The interaction with phonons shifts the bottom of the ground-state band of the  $j$ -th carrier in the QW by  $\Delta$ . Hence, the exciton ground-state energy in a nanofilm with thickness  $a$  and at the temperature  $T$ , after being renormalized by the interaction with phonons, is determined by the expression [21]

$$E_{\text{ex}}(a, T) = E_{\text{ex}}^{(0)}(a) + \Delta_e(a, T) + \Delta_h(a, T). \quad (4)$$

In the weak-coupling approximation, the bottom shift of the carrier miniband in the QW is determined by the one-phonon mass operator of Green's function at any temperature [18] and is expressed as a sum of partial shifts associated with the interaction with every phonon branch:

$$\Delta(a, T) = \Delta_{L0}(a, T) + \Delta_{L1}(a, T) + \Delta_I(a, T). \quad (5)$$

Analytical expressions for the partial contributions to the total shift (5) can be found in work [21]. The temperature dependence of the shifts of the charge carrier energy levels, in accordance with Eq. (4), is responsible for the appearance of this dependence for the exciton energy.

The parameters required for the calculation of carrier energies in the QW are the QW depth  $V_j$ , effective mass of a charge carrier in the barrier medium  $m_j^{(1)}$ , and energy of a semiconfined phonon  $\Omega_{L1}$ . All of them and, therefore, the efficiency of the phonon interaction with charge carriers depend on the aluminum content  $x$ :

$$\begin{aligned}
 V_j &= A_j(1.115x + 0.37x^2) \text{ (eV)}, \\
 m_e^{(1)} &= (0.067 + 0.083x)m_e, \\
 m_h^{(1)} &= (0.62 + 0.14x)m_e, \\
 \Omega_{L1} &= 36.25 + 1.83x + 17.12x^2 - 5.11x^3 \text{ (meV)}
 \end{aligned}$$

Here,  $m_e$  is the rest mass of a free electron,  $A_e = 0.6$ ,  $A_h = 0.4$ , and  $0 \leq x \leq 1$ . Therefore, the energy of an exciton in the nanofilm also turns out to depend parametrically on  $x$ . The dependences presented above were obtained in work [24] by analyzing and interpolating the results of experimental measurements carried out for some physical parameters of  $\text{Al}_x\text{Ga}_{1-x}\text{As}/\text{GaAs}$  heterostructures. Being used at the calculation of the exciton binding energy in the quantum wells on the basis of  $\text{Al}_x\text{Ga}_{1-x}\text{As}/\text{GaAs}$  with  $x$  varying from 0.1 to 0.6, they brought about results that agree well with the data of experimental measurements [25].

This work aimed at studying the dependence of the exciton energy (4) on the nanofilm thickness and the temperature at various aluminum contents in the barrier medium.

### 3. Results and Their Discussion

Specific calculations were carried out, by using the  $\text{Al}_x\text{Ga}_{1-x}\text{As}/\text{GaAs}/\text{Al}_x\text{Ga}_{1-x}\text{As}$  nanofilms with  $x = 0.2, 0.3$ , and  $0.4$  as an example. The analysis of corresponding results obtained in the case  $T = 0$  K shows that the partial contribution to the bottom shift (5) of the charge carrier ground-state miniband associated with the interaction between a charge carrier and confined phonons ( $\Delta_{L0}$ ) is a monotonically and nonlinearly growing function of the nanofilm thickness (Fig. 1). The growth rate of this function is maximum in the interval  $a < 20$  nm for the electron and  $a < 10$  nm for the hole, but its dependence on the content  $x$  is nonmonotonic. The increase in  $x$  results in the growth of the partial contribution associated with the interaction between the electron (hole) and confined phonons, if the nanofilm thickness is smaller

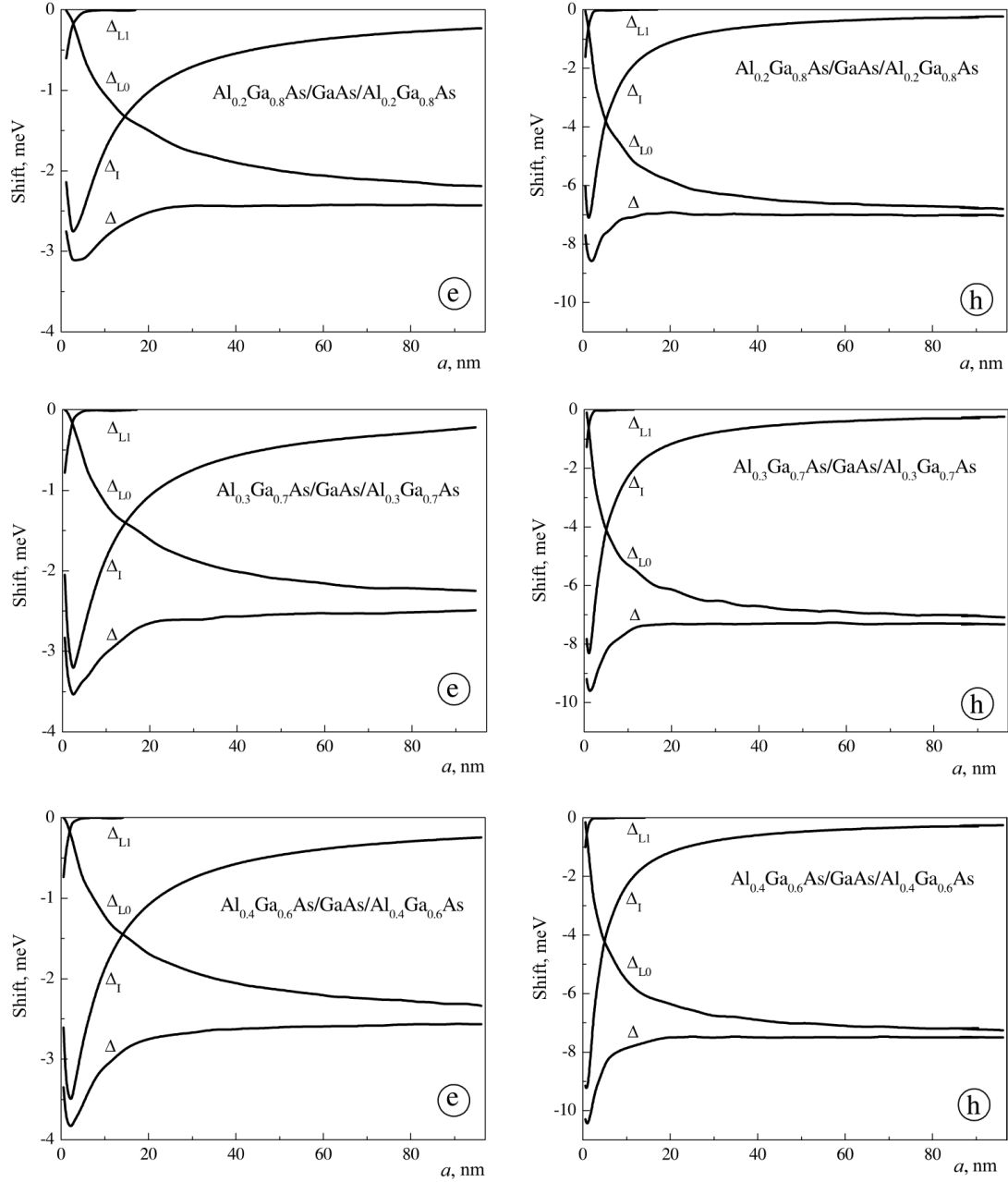


**Fig. 1.** Dependences of the partial ( $\Delta_{L0}$ ,  $\Delta_{L1}$ ,  $\Delta_I$ ) and total ( $\Delta$ ) shifts of the bottoms of the electron (e) and hole (h) ground-state minibands on the nanofilm thickness  $a$  at  $T = 0$  and various  $x = 0.2, 0.3$ , and  $0.4$  (from top to bottom)

than 10 nm (5 nm), and in a reduction of this contribution, if  $a$  is larger. In the nanofilms more than 50 nm in thickness, the magnitude of  $\Delta_{L0}$  is no more sensitive to the variation of  $x$ , by approaching, at  $a \geq 100$  nm, a value of 2.9 meV (8.8 meV) typical of

the energy of an electron (hole) polaron in a massive GaAs crystal.

Owing to the symmetry of the ground-state wave function of charge carriers in the QW, only their interaction with the symmetric branch of  $I$ -phonons is

relevant. An increase in the aluminum content in the barrier medium strengthens the interaction with  $I$ -phonons as a result of both their energy growth and the growth in the magnitude of electron-phonon coupling function [15], because the difference between the values of dielectric permittivities in the well and the barrier medium increases at that.

The magnitude of  $\Delta_{L1}$  is mainly formed by the interaction between semiconfined phonons and the electron states in the ground-state miniband, and, similarly to  $\Delta_I$ , drastically decreases, if the nanofilm thickness grows. In this case, the dependence of  $\Delta_{L1}$ , unlike  $\Delta_I$ , on  $a$  turns out monotonically descending, and its initial values are much smaller than those of  $\Delta_I$ . In contrast to  $\Delta_I$  and  $\Delta_{L0}$ , the partial contribution  $\Delta_{L1}$  decreases, as the content  $x$  increases. This behavior is explained by the growth of the QW depth and the corresponding reduction of the probability for the electron to penetrate into the barrier medium and, hence, by a decrease in its coupling with those phonons.

The indicated behavior demonstrated by the dependences of the partial contributions associated with the electron (hole) coupling with semiconfined and interface phonons on the nanofilm thickness and the barrier material composition is responsible for their substantial changes, as the parameter  $x$  varies for films with the thickness to 5 nm (2.5 nm) and 60 nm (30) nm, respectively.

The results of our research concerning the temperature dependences of the shifts of the electron and hole ground-state miniband bottoms, which were calculated, by using formula (5) for several fixed values of nanofilm thickness  $a$  (expressed in terms of GaAs monolayer units), are exhibited in Fig. 2. It is evident that the character of temperature-induced variations of the total shift  $\Delta$  is different for nanofilms with different thicknesses and different aluminum contents. This fact is explained by the features in the interaction of an electron with interface phonons. Namely, the shift component  $\Delta_I$  governed by the processes of phonon absorption [21] can be positive or negative, depending on the number of levels in the QW and the distance between them, which is determined by the nanofilm thickness. The origin of why the sign may change is a peculiarity in the dependence of the function describing the coupling between the electron state in the QW and  $I$ -phonons on the quasimomentum: its maximum can be located in the

intervals of small or large quasimomentum values, depending on the nanofilm thickness and the state energy. As a result, the interaction with phonons is effective for charge carriers with small or large kinetic energies in comparison with the phonon energy. The manifestations of this interaction are diverse: it is most probable that low-energy quasiparticles will obtain the energy from the phonon system, whereas high-energy ones will lose it. Each of those processes stimulates a shift of the band bottom in the opposite direction. The number of levels in the QW, their positions, and the distances between them are changed, if the nanofilm thickness varies. Accordingly, the influence of processes with absorption and emission of  $I$ -phonons of low- and high-energy types also changes. It is the nonmonotonic behavior of those influences within the interval of nanofilm thickness changes that is responsible for the indicated difference between the temperature dependences of partial contributions made by interface phonons [21].

The dependences of the bottom shifts of the electron and hole ground-state minibands on the nanofilm thickness  $a$  at various fixed temperatures  $T$  are plotted in Fig. 3. One can see that, as the nanofilm thickness increases, the bottom of the ground-state miniband shifts toward smaller energies, by nonmonotonically reaching a maximum in ultrathin films; at  $a > 20$  nm, the character of the curves remains similar to that of curves shown in Fig. 1. This fact is explained by the character of the corresponding partial shift changes caused by the interactions with  $L0$ -,  $L1$ -, and  $I$ -phonons. The growth of the nanofilm temperature strengthens the height of the maximum and shifts it toward larger thicknesses, with the position and the initial height (at  $T = 0$ ) of the maximum depending on  $x$  (Fig. 1).

The changes in the electron and hole energies give rise to the corresponding shifts of the bottom energy of the exciton ground-state miniband,

$$\Delta_{\text{ex}}(a, T) = \Delta_e(a, T) + \Delta_h(a, T). \quad (6)$$

The dependence of the shift  $\Delta_{\text{ex}}$  on the temperature (Fig. 4) turns out a monotonic function. For ultrathin films, its character depends on both the film thickness and the aluminum content (see curves  $N = 2$  in Fig. 4). In nanofilms thicker than 40 ML(GaAs), the shift grows, as the temperature increases at a rate

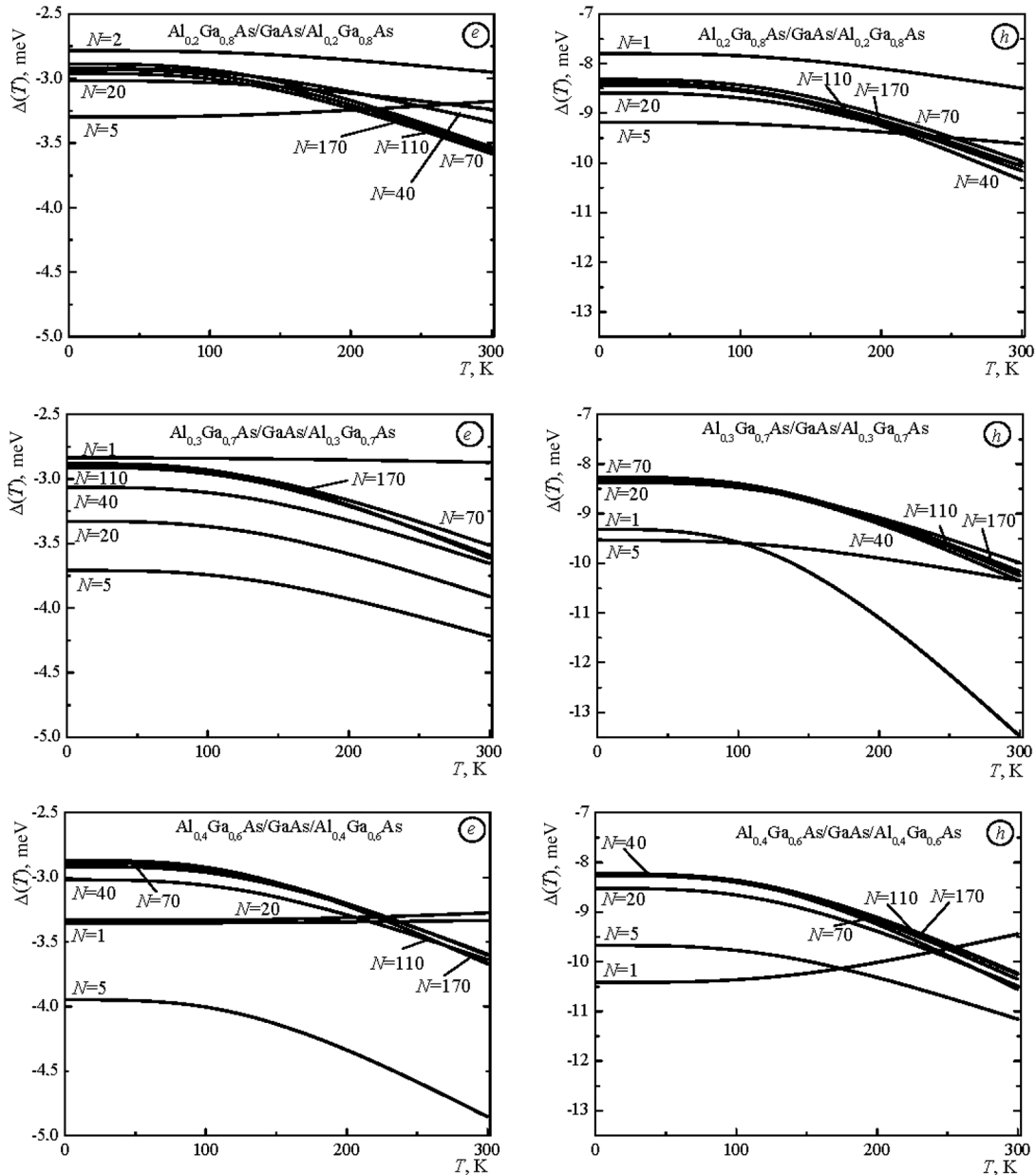


**Fig. 2.** Dependence of the shifts  $\Delta$  of the bottoms of the electron (*e*) and hole (*h*) ground-state minibands owing to the coupling with optical phonons on the temperature  $T$  for various nanofilm thicknesses  $N$  and contents  $x = 0.2, 0.3,$  and  $0.4$  (from top to bottom)

that increases, as the aluminum content in the barrier material grows.

The plots of the dependences of  $\Delta_{\text{ex}}$  on the nanofilm thickness at fixed  $x$  and  $T$  values (see Fig. 5) are similar to those depicted in Fig. 3. The temperature growth stimulates the growth of the shift: the

higher the content, the larger is the shift. The rate of temperature-induced growth is different in different intervals of the nanofilm thickness and for different contents. In superthin (less than 10 nm) films, it is governed by the interaction with  $I$ - and  $L1$ -phonons; in thin (up to 30 nm) films, with  $I$ - and  $L0$ -phonons;

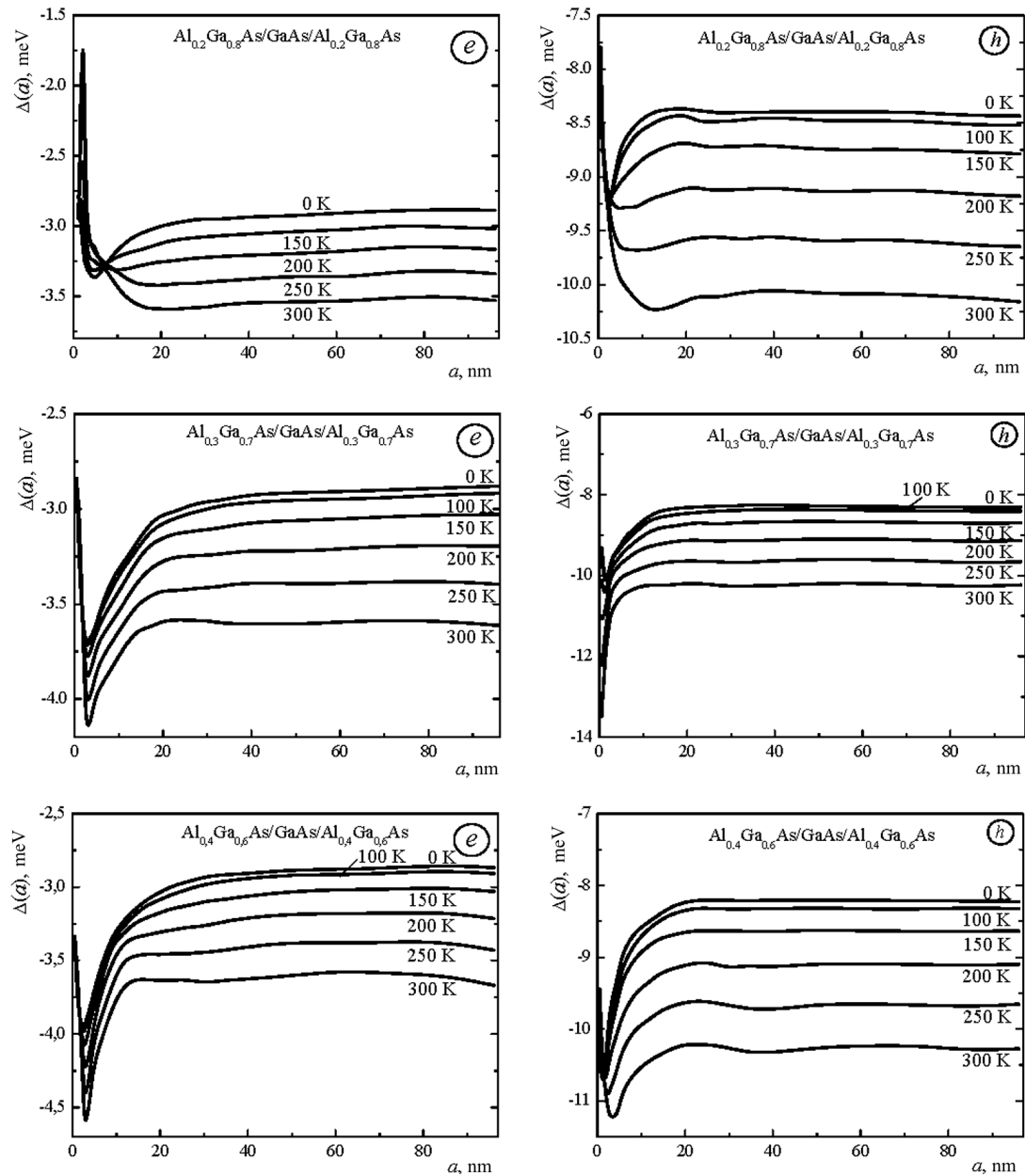


**Fig. 3.** Dependence of the shifts  $\Delta$  of the bottoms of the electron (e) and hole (h) ground-state minibands owing to the coupling with optical phonons on the nanofilm thickness  $a$  for various temperatures (indicated near the corresponding curves) and contents  $x = 0.2, 0.3,$  and  $0.4$  (from top to bottom)

and in thicker films, mainly with  $L0$ -phonons. The coupling functions for  $I$ - and  $L1$ -phonons depend on the content explicitly in terms of the effective masses, dielectric permittivities, and energies of those phonons. In the case of  $L0$ -phonons, this dependence is implicit, in terms of the electron (hole) wave vec-

tor, which is determined by the depth of the corresponding QW; the latter, in turn, changes if the content  $x$  varies. As the results of calculations show, the nanofilm temperature growth from 0 to 300 K results in an enhancement of the exciton band bottom shift. If  $x = 0.2$ , the shift changes from 12 to

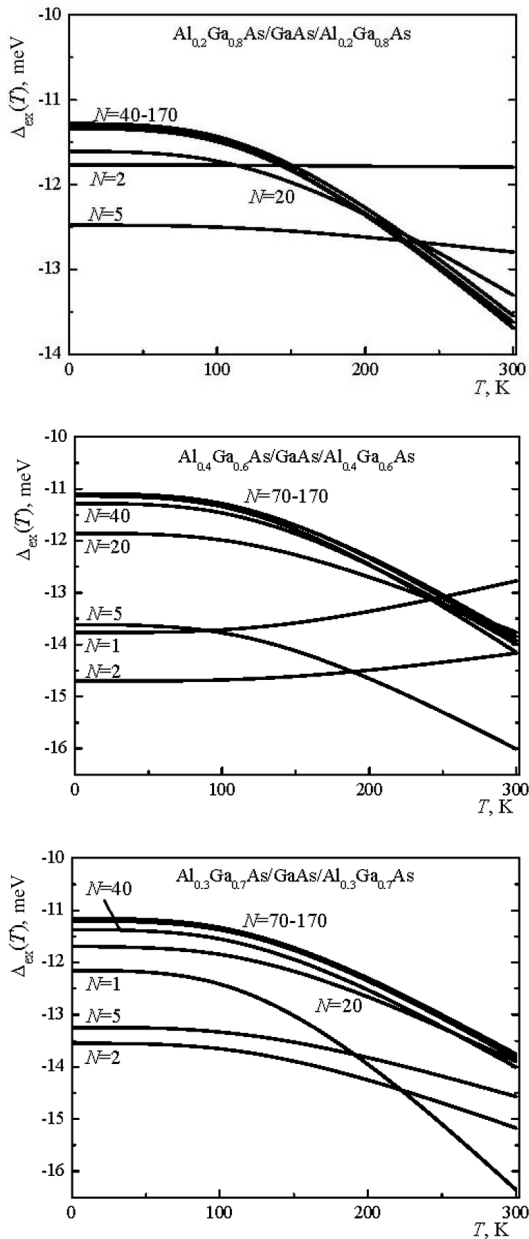


**Fig. 4.** Shift of the exciton ground-state level induced by the coupling with optical phonons as a function of the nanofilm thickness  $a$  at fixed temperatures  $T$  and contents  $x$

13.7 meV at  $a \leq 5$  nm and from 11.3 to 14 MeV at  $a \geq 100$  nm; if  $x = 0.3$ , from 13.6 to 16.5 meV and from 11.2 to 13.8 meV, respectively; and if  $x = 0.4$ , from 14 to 16 meV and from 11 to 14 meV, respectively.

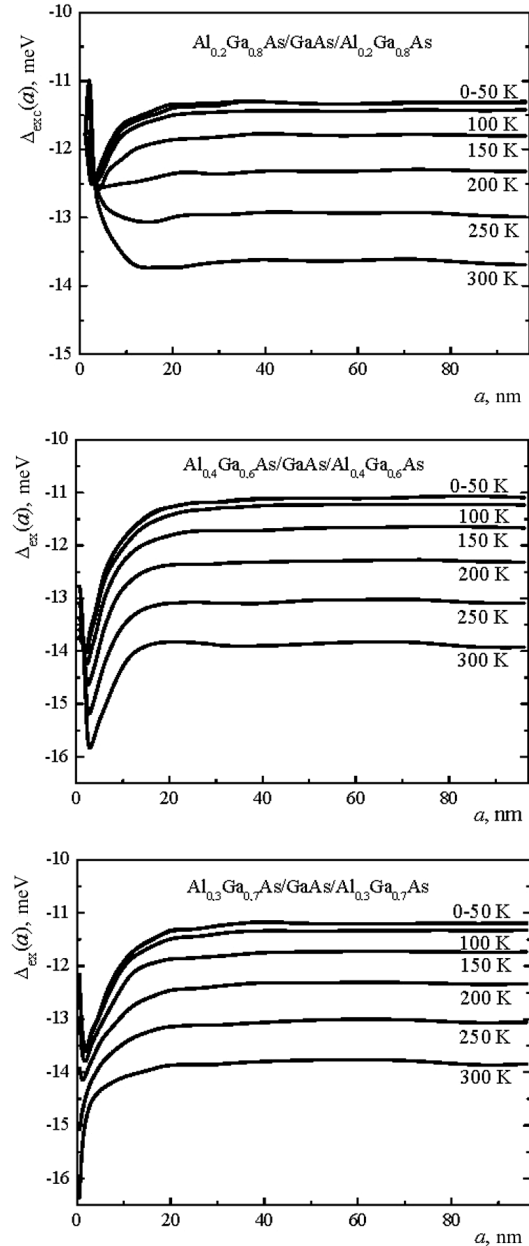


**Fig. 5.** Shift of the exciton ground-state level as a function of the temperature  $T$  at fixed nanofilm thicknesses  $a$  and contents  $x$

The results of calculations for the dependences of the excitonic transition energy on the nanofilm thickness at various temperatures and barrier material contents are exhibited in Fig. 6. They testify that the reduction of the film thickness to 37 ... 33 nm re-



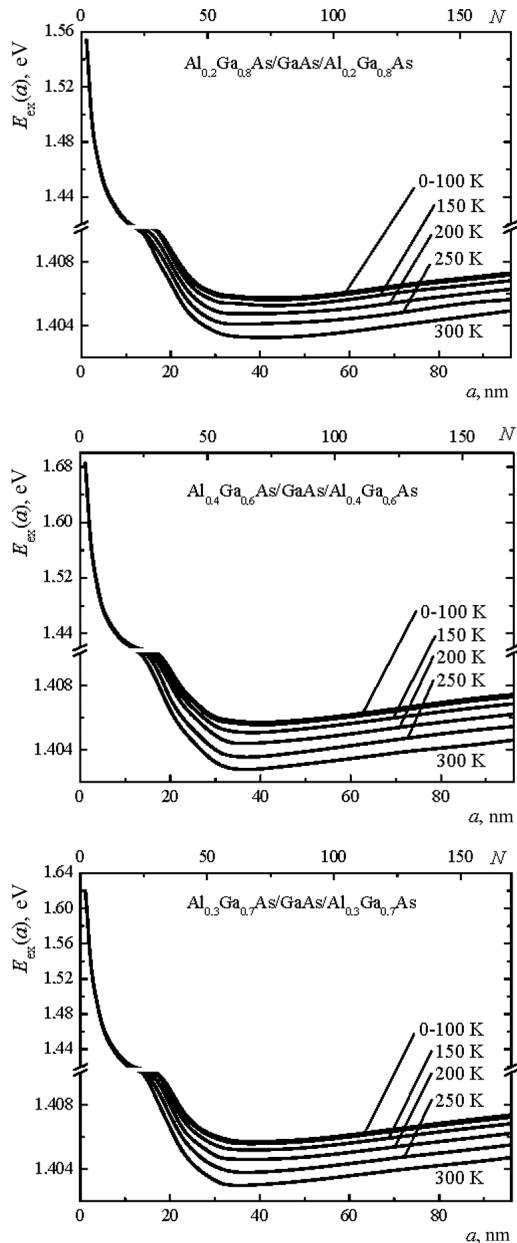


**Fig. 6.** Energy of the exciton transition into the ground state as a function of the nanofilm thickness at fixed temperatures  $T$  and various contents  $x$

sults in a decrease of  $E_{\text{ex}}$ , which is stronger for higher temperatures. This reduction is related to the corresponding growth of the exciton binding energy by approximately 5 meV. The further reduction of the nanofilm thickness results in a steeper growth of the transition energy, mainly as a result of the influence

of the size confinement effects, which give rise to a shift of the electron and hole levels in their QWs. The temperature increase lowers the transition energy by 2–3 meV, depending on  $x$ .

#### 4. Conclusions

The analysis of the results obtained in our research testifies to the nonlinear dependence of the exciton transition energy on the nanofilm thickness. When the latter increases to 30–40 nm, the value of  $E_{\text{ex}}$  drastically decreases at  $T = 0$  K from 1.55 eV at  $x = 0.2$ , 1.62 eV at  $x = 0.3$ , and 1.69 eV at  $x = 0.4$  to 1.41 eV for all those contents, mainly as a result of the weakening of the size confinement effect. The further increase of the nanofilm thickness to approximately 100 nm is accompanied by a slow growth of  $E_{\text{ex}}$  to a value characteristic of massive GaAs crystals. This growth occurs mainly as a result of the reduction of the exciton binding energy, and the rate of this growth weakly depends on  $x$ . The temperature elevation from 0 to 300 K stimulates a long-wave shift of the exciton band bottom, which gives rise to a reduction of  $E_{\text{ex}}$  by a value of about 2 meV at  $x = 0.2$  and 3 meV at  $x = 0.4$ , which weakly depends on the nanofilm thickness. The temperature-induced variations originate from the coupling with phonons; the latter are mainly confined ones in nanofilms thicker than 30–40 nm (the exact value depends on  $x$ ) and interface ones in thinner films.

1. E.L. Ivchenko and G.E. Pikus, *Superlattices and Other Heterostructures: Symmetry and Optical Phenomena* (Springer, Berlin, 1995).
2. E.L. Ivchenko, in *Optics of Nanostructures*, edited by A.V. Fedorov (Nedra, St.-Petersburg, 2005), p. 105 (in Russian).
3. I.I. Zasavitsky, D.A. Pashkeev, A.A. Marmalyuk *et al.*, *Kvant. Elektron.* **40**, 95 (2010).
4. V. Shchukin, N.N. Ledentsov, and D. Bimberg, *Epitaxy of Nanostructures* (Springer, Berlin, 2004).
5. A.B. Krysa, J.S. Roberts, R.P. Green *et al.*, *J. Cryst. Growth* **272**, 682 (2004).
6. M.J. Manfra, arXiv:1309.2717 (2013).
7. S. Zybell, H. Schneider, S. Winnerl *et al.*, *Appl. Phys. Lett.* **99**, 041103 (2011).
8. W. Lu, N. Li, S.C. Shen *et al.*, in *Proceedings of the 25th International Conference on Infrared and Millimeter Waves, Beijing, China, Sept. 12–15, 2000*, p. 37.

9. S. Krukovskiy, B. Koman, and N. Strukhlyak, *Visn. Lviv. Univ. Ser. Fiz.* **38**, 276 (2005).
10. D.M.Zayachuk, S.I. Krukovskiy, I.O. Mrykhin *et al.*, *Fiz. Khim. Tverd. Tila* **6**, 661 (2005).
11. T. Sarkr and S.K. Mazumder, *IEEE Trans. Electron Devices* **54**, 589 (2007).
12. A. Weerasekara, S. Matsik, M. Rinzan *et al.*, *Opt. Lett.* **32**, 1335 (2007).
13. L. Wendler and R. Pechstedt, *Phys. Status Solidi B* **141**, 129 (1987).
14. K. Huang and B.F. Zhu, *Phys. Rev. B* **38**, 13377 (1988).
15. N. Mori and T. Ando, *Phys. Rev. B* **40**, 6175 (1989).
16. G.Q. Hai, F.M. Peeters, and J.T. Devreese, *Phys. Rev. B* **48**, 4666 (1993).
17. A. Thilagam and J. Singh, *Appl. Phys. A* **62**, 445 (1996).
18. M.V. Tkach, *Quasiparticles in Nanoheterosystems. Quantum Dots and Wires* (Ruta, Chernivtsi, 2003) (in Ukrainian).
19. V.I. Boichuk, V.A. Borusevych, and I.S. Shevchuk, *J. Optoelectron. Adv. Mater.* **10**, 1357 (2008).
20. V.M. Kramar and M.V. Tkach, *Ukr. Fiz. Zh.* **54**, 1029 (2009).
21. V.M. Kramar, *Ukr. Fiz. Zh.* **54**, 1226 (2008).
22. W. Trzeciakowski and B.D. McCombe, *Appl. Phys. Lett.* **55**, 891 (1989).
23. Q.X. Zhao, S. Wongmanerod, M. Willander *et al.*, *Phys. Rev. B* **62**, 10984 (2000).
24. S. Adachi, *J. Appl. Phys.* **58**, R1 (1985).
25. R. Zheng and M. Matsuura, *Phys. Rev. B* **58**, 10769 (1998).

Received 20.06.14.

Translated from Ukrainian by O.I. Voitenko

*Д.В. Кондрюк, В.М. Крамар*

ЗАЛЕЖНІСТЬ ЕНЕРГІЇ  
ЕКСИТОННИХ ПЕРЕХОДІВ У НАНОПЛІВКАХ  
 $\text{Al}_x\text{Ga}_{1-x}\text{As}/\text{GaAs}/\text{Al}_x\text{Ga}_{1-x}\text{As}$  ВІД ТОВЩИНИ,  
КОНЦЕНТРАЦІЇ ТА ТЕМПЕРАТУРИ

Резюме

У наближенні діелектричного континууму методом функцій Гріна досліджено залежність енергії переходу в основний екситонний стан квазідвовимірної плоскої напівпровідникової наногетероструктури з одиночною квантовою ямою — наноплівки від її товщини, температури та складу бар'єрного середовища. Конкретний розрахунок здійснено на прикладі наноплівки з прямокутною, скінченної глибини, квантовою ямою, створеною подвійним гетеропереходом  $\text{GaAs}/\text{Al}_x\text{Ga}_{1-x}\text{As}$ . Показано, що в плівках товщиною до 30–40 нм величина енергії переходу визначається переважно впливом просторового обмеження та концентрацією алюмінію  $x$  — стрімко зменшується при зростанні товщини від 1,55 (при  $x = 0,2$ ), 1,62 (при  $x = 0,3$ ) і 1,69 (при  $x = 0,4$ ) еВ до 1,41 еВ для усіх наведених значень  $x$ . Подальше збільшення товщини плівки приблизно до 100 нм супроводжується повільним зростанням енергії переходу до значення, характерного для масивного  $\text{GaAs}$ , переважно внаслідок зменшення енергії зв'язку екситону; швидкість цього зростання слабо залежить від  $x$ . Збільшення температури від 0 до 300 К викликає довгохвильове зміщення дна екситонної зони, що зумовлює зменшення енергії переходу на слабо залежну від товщини плівки величину, яка становить приблизно 2 меВ при  $x = 0,2$  та 3 меВ при  $x = 0,4$ . Причиною температурних змін є взаємодія з фононами, переважно обмеженими у наноплівках товщиною понад 30–40 нм, залежно від  $x$ , та інтерфейсними — у тонших.